



Original

Gan, W.; Huang, Y.; Xu, Y.; Hofmann, M.; Kainer, K.; Hort, N.:

In Situ Tensile Texture Analysis of a New Mg-RE Alloy.

In: Sommitsch C.; Ionescu M.; Mishra B.; Mishra B.; Kozeschnik E.; Chandra T. (eds.): Materials Science Forum. Vol. 879 Zürich-Stafa: Trans Tech Publications, 2017. 779 – 783.

First published online by Trans Tech Publications: November 2016

<https://dx.doi.org/10.4028/www.scientific.net/MSF.879.779>

***In Situ* Tensile Texture Analysis of a New Mg-RE Alloy**

Weimin Gan¹, Yuanding Huang^{2,*}, Yuling Xu², Michael Hofmann³,
Karl Ulrich Kainer² and Nobert Hort²

¹German Engineering Materials Science Centre at MLZ, Helmholtz-Centre Geesthacht,
D-85748, Garching, Germany

²Magnesium Innovation Centre, Helmholtz-Centre Geesthacht, D-21502, Geesthacht, Germany

³Heinz Maier-Leibnitz Zentrum (MLZ), Technische Universität München,
D-85748 Garching, Germany

Keywords: Magnesium alloy, texture, *in-situ*, neutron diffraction

Abstract. A new Mg-RE (rare earth) alloy was previously developed by micro-alloying method (RE < 0.4 wt.%), which achieves a high ductility and good corrosion resistance. *In-situ* tensile test via neutron and synchrotron diffraction were performed to investigate first the deformation behaviour; and second the texture evolution which can be related to the deformation mechanism, and finally to understand why the as-cast Mg-RE alloys show such a high tensile ductility.

Preliminary results showed that a dominated basal fibre texture was gradually developed with the increase of tensile strain. However, before the sample was broken a (10.0) fibre texture showed a similar intensity to that in (00.2), which means more activations of the non-basal slip planes during tensile deformation. This could also contribute to a relatively high elongation of this new Mg-RE alloy at room temperature. Further discussion will be showed together with the microstructures.

Introduction

The applications of magnesium alloys have been increasing now days, because they are not only developed as structural materials for transportation or other industrial applications, but also as biodegradable medical implant materials [1]. However, Mg alloys exhibit relatively low ductility due to their *h.c.p.* crystallographic structure which has limited available activation dislocation systems at room temperature. Efforts have been dedicated to improve the mechanical property of Mg and its alloys by means of alloying design or grain refinement on the as-cast ingot through thermo-mechanical deformation, such as extrusion, rolling, et al., and advanced severe plastic deformation (SPD) techniques (e. g., ECAP, ARB, HPT, and etc.) [2- 4].

The rare-earth metals have active chemical properties, being the most potential alloying elements for Mg alloy, because they can play important roles in getting rid of impurities and improving the performance of Mg-RE alloys [5] A concept of multi-micro-alloying by REs (< 0.4 wt. %) was introduced to develop wrought Mg alloys [6], which is very attractive because of its low cost. Researches have shown that addition of RE to Mg, such as Y- yttrium, Nd- neodymium, Gd- gadolinium, Dy- dysprosium, etc., can also decrease the susceptibility to micro porosity during casting and contributes to its following hot extrusion or rolling process. Relatively high ductile Mg-RE alloys over conventional AZ and ZK series Mg alloys were obtained [7]. The addition of RE contributes to the improvement of mechanical properties and as well the corrosion resistance [1, 8]. While the real activation mechanisms in Mg-RE is still unclear.

It is known that there are a various possibilities of deformation mechanisms in Mg: the basal slip, non-basal slips, deformation twinning and grain boundary sliding (GBS), but only two independent slip systems (basal slips) are easily activated at room temperature. To fulfil the von Mises' criterion which requires five independent deformation modes during plastic deformation of polycrystals, strain along the <0001> axis in *h.c.p.* metals can be accommodated by twinning and 1/3 <11-23> <c+a> slip [9]. There are typically two deformation twin modes for Mg: one is the {10-12} <10-11> c-axis tension twin and the other is the {10-11} <10-12> c-axis compression twin [10, 11]. The former tends

to be generated at the onset of plastic deformation and contributes to straining; on the other hand, the latter often occurs at a later or the final stage of deformation and relaxes the stress concentration.

Less activation of dislocation system in Mg easily leads to strong anisotropy, i.e. the formation of preferred orientation/ texture. Typical texture developed under thermo-mechanical deformation or annealing of Mg and its alloys has been well reported and documented [12]. Study on the texture evolution can help to understand the dislocation activation system. Diffractions for *in-situ* microstructural analysis, such as lattice strain and texture, using advanced neutron facilities take more advantages because they offer a high penetration depth and a relatively fast data collection with area detector. Such kind of diffractometers equipped with load frames or furnace are well developed in current days and are still in proving [13]. Since crystallographic texture measurement is time consuming high flux neutron measurements at successive points of the strain-stress curve under tensile or compression allows describing the texture evolution. Fundamentals of the pole figure measurement using neutron diffraction has been described [14]. *In-situ* texture analysis according to the stress-strain curve can contribute to confirm the simulation of texture and mechanical property evolution via tensile or compression experiments.

A relatively high ductility Mg-Gd-Zr (in as-cast state) was developed using micro-alloy method in our previous work [6]. Current study is aimed to investigate the tensile deformation behaviour of this new alloy via *in-situ* neutron diffraction; and to further understand the fundamental of high plasticity of this alloy through bulk texture analysis.

Experimental procedure

Materials. The Mg-0.4Gd-0.5Zr alloy was prepared in steel crucible under a cover gas mixture of CO₂ and SF₆. After stirring at 730 °C for 0.5 h, the alloy was cast to the mould preheated at 500 °C. The filled mould was held at 670 °C for 30 min. under the protective gas to let the heavy impurities settle to the bottom and the light impurities float up to the top of the ingots. Then the permanent mold direct chill casting was used to prepare the alloys. Thereafter, the whole steel crucible with the melt was immersed into the continuous cooling water at a speed of 20 mm·s⁻¹. As soon as the liquid level of inside melt was aligned with the height of outside water, the solidification process was finished. The weight of the obtained ingot was about 2 kg. The detailed chemical composition of this alloy analysed by x-ray fluorescence spectrometer was Mg- 0.38 wt.% Gd- 0.20 wt.% Zr (Mg04GdZr).

***In-situ* pole figure measurement.** Tensile specimen with a dimension of Ø6×35 mm was machined from the ingot. *In-situ* experiment was performed at the neutron diffractometer STRESS-SPEC at FRM II (Heinz Maier-Leibnitz Zentrum, Garching, Germany) using a novel tensile rig [15]. The used wavelength was 1.748 Å from Ge (311) monochromator. The investigated gauge volume was 5×5×5 mm³ controlled by a primary slit and a radial collimator in front of the detector, as shown in Fig. 1. The texture measurement points were selected to some specific loads, i.e. under yield strength, strain hardening, hardening to platform transition, UTS and broken. At each point the specimen was first pulled to a fixed load under a speed of 3.5 N/s; and then simultaneously fixed the position when reaching the load. Pole figure measurement was done using non-continuous phi rotation with 40 s per 5°. Measured complete pole figures were calculated from 2D area detector images using SteCa software [16]. The measured pole figures were used to calculate ODFs and inverse pole figures based on the series expansion method by Bunge with a expansion degree $L_{max}=30$ [17].

Results and discussion

Fig.2 shows the optical microstructures (OM) of the as-cast pure Mg and Mg-Gd-Zr alloy, respectively. Clear is that the grains of the Mg-Gd-Zr alloy was greatly refined. Fig. 2(c) presents the room temperature curves of these two materials. Very large increase of both tensile stress and ductility can be directly seen from the figure. The *in-situ* pole figure measurement points during tensile test are marked as P1 to P5 whose stress and strain values are listed in Fig. 3.

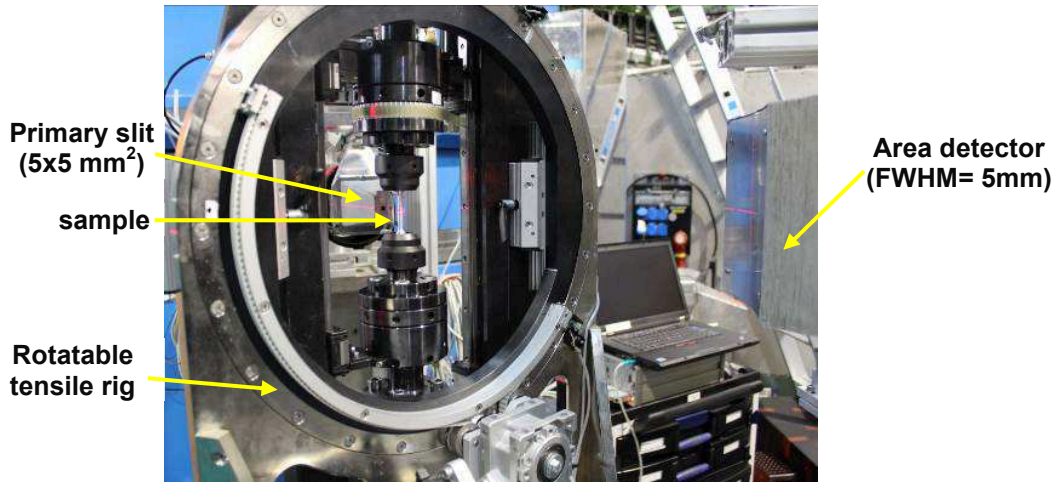


Fig. 1 Rotatable tensile rig at STRESS-SPEC for *in-situ* pole figure measurement via tensile.

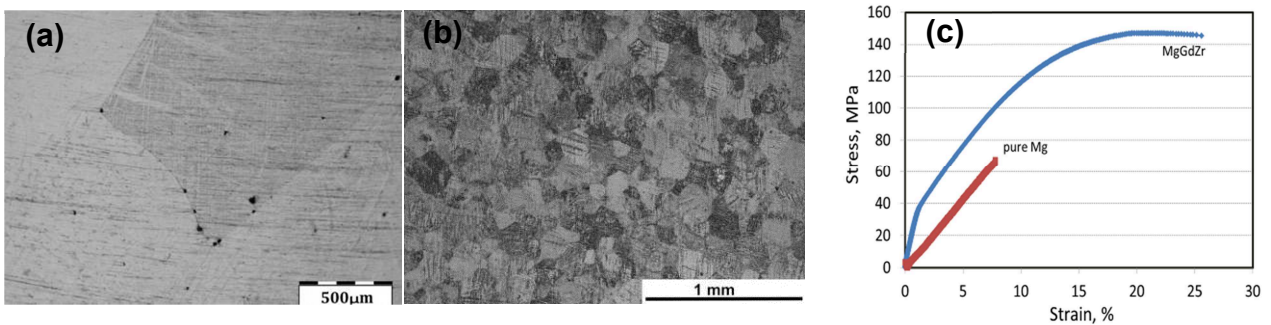


Fig. 2 OM microstructures of the as-cast pure Mg (a) and the as-cast Mg-Gd-Zr alloy (b); and their room temperature tensile curves (c), respectively.

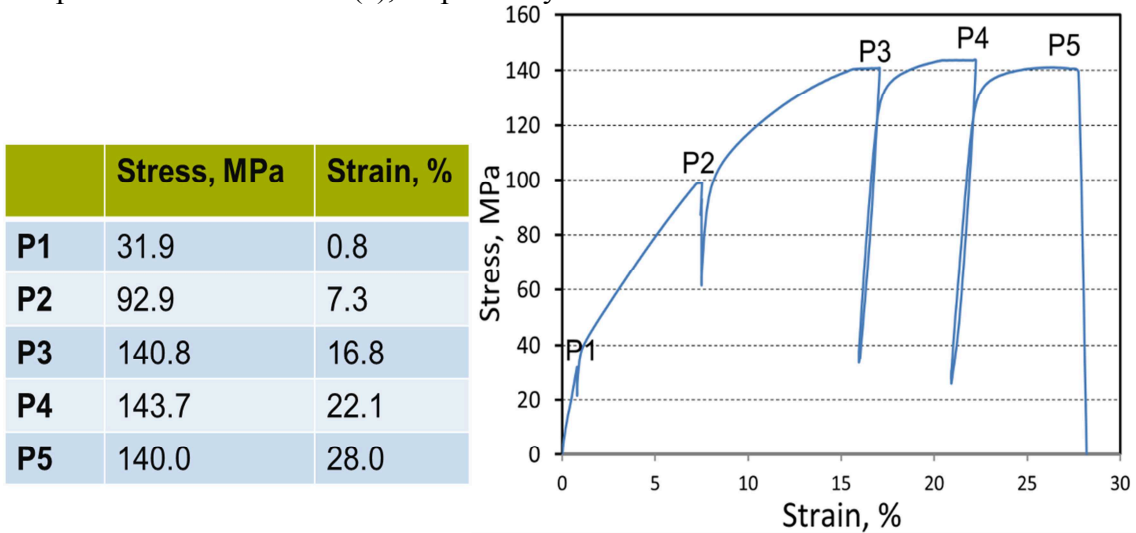


Fig. 3 *In-situ* pole figure measured points P1 to P5 in the tensile curve.

Fig. 4 illustrates the (10.0) and (00.2) measured complete pole figures of the P1 to P5, respectively. At P1 a random distribution is observed. At P2 where the sample was tensioned to a strain of 7.3% the basal planes of most grains are re-oriented to be parallel to the tensile direction (in the pole figure centre), i.e. the formation of a (10.0) fibre. Further increase of tensile strain to P3 and P4 the pole figures show no obvious change but a slight increase of maximum pole intensity. After broken at P5 similar as a shear component is evident. This should be due to an instantaneous torsion effect.

To obtain more details the calculated inverse pole figures which are parallel to the tensile direction of the five points are successively shown in Fig. 5. A standard inverse pole figure in which conventional pole components are marked is also presented. First, the strengthening of the (10.0) fibre from P2 to P5 is obvious. Second, non-basal components like (11.2) and (21.3) are obtained

from P2 to P5. This indicates the activations of non-basal plan sliding during tensile deformation. Moreover, optical microstructures of the pole figure measurement points are also shown in Fig. 6. It is noted that there exists many twins in all the cases, which indicates that the twinning deformation is very active during the whole tensile deformation.

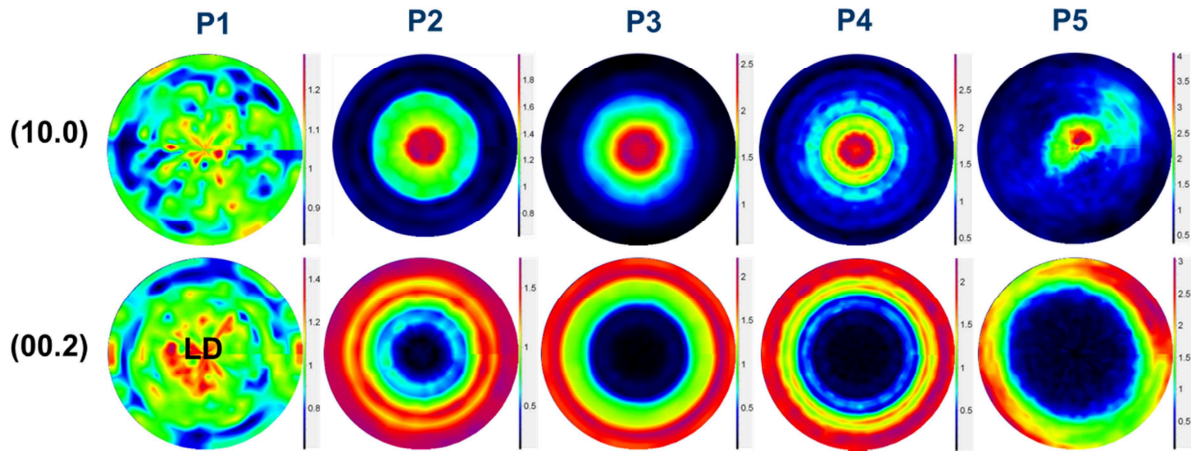


Fig. 4 (10.0) and (00.2) pole figure evolution of the P1 to P5 (tensile direction is in the pole figure centre).

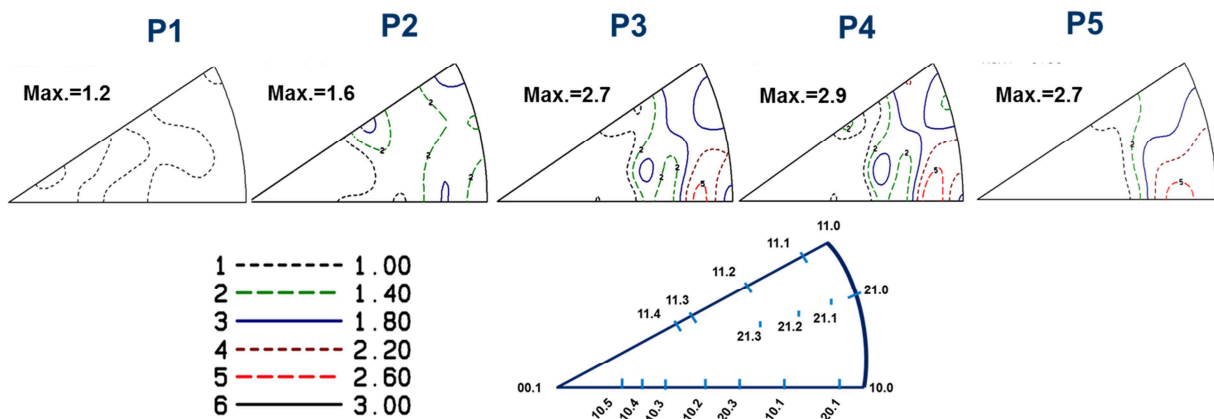


Fig. 5 Evolution of inverse pole figure which is parallel to the load/tensile direction of the P1 to P5.

Combining the texture and microstructure evolutions which are presented above the tensile deformation behaviour of the Mg-Gd-Zr alloy can be described as follows. The strong hardening from P1 to P2 in the tensile curve could be mainly due to the basal sliding and twinning deformation. While at P3 and P4 points where a plateau occurs in the tensile curve some activation of non-basal planes is expected, which contributes a lot to the increase of the ductility of this new Mg-Gd-Zr alloy. It should be also pointed out that the quantitative texture simulation can offer more details since similar studies have been done in conventional Mg alloys based on a VPSC model [18- 20]. This work is currently in progress.

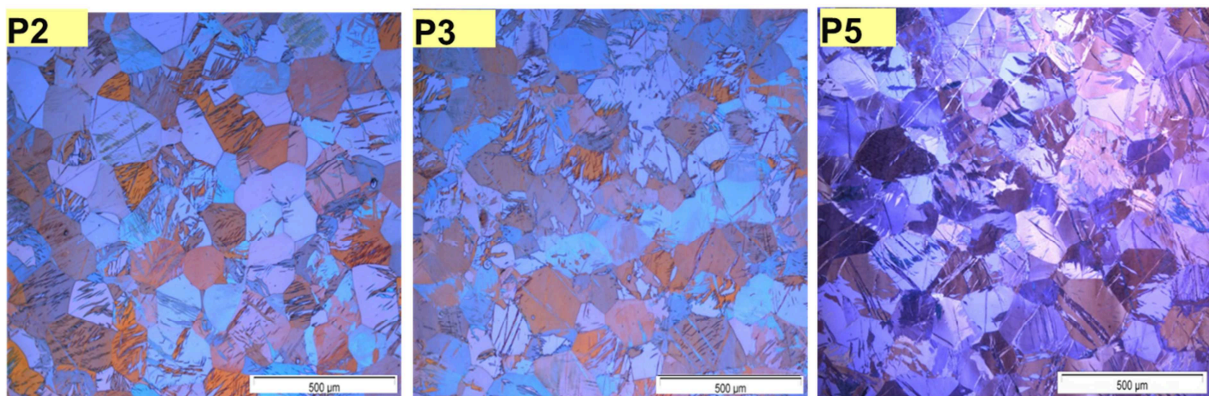


Fig. 6 OM microstructures at the pole figure measurement points P2, P3 and P5, respectively.

Summary

The bulk pole figures at five points of a new Mg-Gd-Zr alloy during tensile deformation were successfully measured *in situ* via neutron diffraction. The produced texture during tensile test has been well correlated to the strain hardening behaviour and microstructure evolution. Results indicated besides the basal sliding and the twinning contribution, non-basal activation plays also an important role, especially at the stage when the strains reach a plateau. This greatly contributes to the high ductility of the new Mg-Gd-Zr alloy in current study.

Acknowledgement

The authors would like to thank the help from K. Braun and Dr. P. Juergen at FRM II in Garching for working on the tensile machine during the neutron beam time.

References

- [1] L. Yang, Y. Huang, F. Feyerabend, R. Willumeit, K.U. Kainer and M. Hort, *J. Mech. Behav. Biomed. Mater.* 13 (2013) 36-44.
- [2] M.B. Yang, H.L. Li, R.J. Cheng, F.S. Pan and H.J. Hu, C.Y. Duan, J. Zhang, *J. Alloys Comp.* 579 (2013) 92-98.
- [3] W.M. Gan, K. Wu, M.Y. Zheng, X.J. Wang, H. Chang, H.-G. Brokmeier, *Mater. Sci. & Eng. A* 516 (2009) 283-289.
- [4] A. Yamashita, Z. Horita and T.G. Langdon, *Mater. Sci. & Eng. A* 300 (2001) 142-147.
- [5] K. Hantzsche, J. Bohlen, J. Wendt, K.U. Kainer, S.B. Yi, D. Letzig, *Scripta Mater.* 63 (2010) 725-730.
- [6] Y.D. Huang, W.M. Gan, K.U. Kainer, N. Hort, *J. Mg & alloys*, 2 (2014) 1-7.
- [7] S. Tekumalla, S. Seetharaman, A. Almajid, M. Gupta, *Metals*, 5 (2015) 1-39.
- [8] A. Srinivasan, C. Blawert, Y. Huang, C.L. Mendis, K.U. Kainer, N. Hort, *J. Mg & alloys*, 3 (2014) 245-256.
- [9] P.G. Partridge, *Metallurg. Rev.* (1967) 169-194.
- [10] M.R. Barnett, *Mater. Sci. & Eng. A* 464 (2007) 1-7.
- [11] M.R. Barnett, *Mater. Sci. & Eng. A* 464 (2007) 8-16.
- [12] Y.N. Wang, J.C. Huang, *Mater. Chem. & Phy.* 81 (2003) 11-26.
- [13] H.-G. Brokmeier, W.M. Gan, C. Randau, M. Voeller, J. Rebelo-Kornmeier, M. Hofmann, *Nucl. Instru. & Meth. in Phy. Res. A* 624 (2011) 87-92.
- [14] H.-G. Brokmeier, *Textures & Micro.* 33 (1999) 13-33.
- [15] M. Hoelzel, W.M. Gan, M. Hofmann, C. Randau, G. Seidl, Ph. Juettner, W.W. Schmahl, *Nucl. Instru. & Meth. in Phy. Res. A* 711 (2013) 101-105.
- [16] C. Randau, U. Garbe, H.-G. Brokmeier, *J. Appl. Cryst.* 44 (2011) 641-646.
- [17] N.J. Park, H.J. Bunge, *Textures & Micro.* 14-18 (1991) 231-240.
- [18] R.A. Lebensohn, C.N. Tome, *Acta Metall. Mater.* 41 (1993) 2611- 2624.
- [19] S.R. Agner, M.H. Yoo, C.N. Tome, *Acta Materialia*, 49 (2001) 4277- 4289.
- [20] S.B. Yi, H.-G. Brokmeier, R.E. Bolmaro, K.U. Kainer, T. Lippmann, *Scripta Materialia*, 51 (2004) 455-460.